

Article

The Prevention and Control Mechanism of Rockburst Hazards and Its Application in the Construction of a Deeply Buried Tunnel

Heng Zhang ¹, Yimo Zhu ¹, Liang Chen ^{2,*}, Weidong Hu ³ and Shougen Chen ¹

¹ Key Laboratory of Transportation Tunnel Engineering, Ministry of Education, Southwest Jiaotong University, Chengdu 610031, China

² School of Civil Engineering, Changsha University of Science and Technology, Changsha 410076, China

³ China Railway SIYUAN Survey and Design Group Co., Ltd., Wuhan 430063, China

* Correspondence: liangchen_2018@163.com

Received: 2 August 2019; Accepted: 29 August 2019; Published: 3 September 2019



Abstract: Rockburst hazards induced by high geostress are particularly prominent during the construction of underground engineering. Prevention and control of rockburst is still a global challenge in the field of geotechnical engineering, which is of great significance. Based on the tunnel group of the Jinping II hydropower station of China, this paper analyzed the mechanical principle of support in the process of construction, and discussed in detail the active release and passive support by numerical simulation and field application. The results show that as two active measures, stress relieve holes and advanced stress relief blasting can release the energy of the microseismic source and transfer the high stress to the deeper surrounding rock, make the surface rock wall with a relatively low stress act as a protective barrier. Their stress release rate is about 12% and 33% in this project, respectively. In term of passive measure, the combined rapid support, which is mainly composed of water swelling anchor and nano-admixture shotcrete, is also an effective way to prevent and control the rockburst under high geostress.

Keywords: deeply buried tunnel; high stress; rockburst characteristics; rockburst damage; numerical simulation; support system

1. Introduction

With the development of transportation and economy, it is inevitable to build long large tunnels in deep underground space [1–5]. At present, the maximum depth of the civil tunnel has exceeded 2500 m. The increasing number of long, large and deep buried tunnels has brought great challenges to the construction and operation of projects [6–12]. However, rockburst is a common problem in the construction of deep tunnels, which occurred widely in Australia [13], Canada [14], South Africa [15,16], China [17–19] and other countries [20–22]. The characteristics of rocks, the magnitude of geositu stress, and the shape of underground engineering will make the phenomena of rockburst different [23,24]. It is a kind of phenomenon that the accumulated elastic deformation potential energy in rock mass suddenly and violently releases under certain conditions, like during or after the excavation of the underground engineering in the high geostress zone, resulting in exfoliation, even the ejection and throw of rock mass [25,26]. Rockburst not only brought great challenges to the construction and advancement of the project, but also seriously threatened the safety of construction personnel and caused huge economic losses. It has always been a worldwide problem in the field of rock underground engineering and rock mechanics [27–29]. Therefore, the prediction and prevention of rockbursts are of great significance to the successful construction in deep-buried underground engineering.

Due to the importance of this problem, considerable research effort, at an international scale has been devoted to the understanding of the rockburst phenomenon. Although the descriptions are inconsistent, the definition, mechanism and classification of rockbursts by scholars are basically the same [30,31]. Hedley and Kaiser et al. [32,33] proposed that a rockburst is defined as damage to an excavation that occurs in a sudden or violent manner and is associated with a seismic event. Stacey [34] noted that a rockburst is a sudden rock failure characterized by rock fragmentation and protrusion from surrounding rock accompanied by a violent release of energy. Linkov [35] presented that the essence of the dynamic phenomena (rockburst) in mines is that the surrounding rock obtains kinetic energy. In terms of prediction, microseismic (MS) technology is a common method for early warning and safety monitoring of underground engineering [36,37]. From the waveform records, the time, location, radiated energy, seismic moment and other source parameters of a seismic event can be obtained. Microseismic technology therefore is a very useful tool for outlining potentially hazardous ground conditions and assisting construction management in effective re-entry decision-making [38–40]. Xu et al. [41] studied the spatiotemporal evolutionary laws of MS events and used MS events and the relationships between MS monitoring information and the excavation process for the Huainan coal mine. Srinivasan et al. [42] used three short-term precursors, namely MS events, MS dissipative energy and predominant signal frequency for rockburst prediction work in the Kolar gold mine of southern India. Li et al. [43] presented a comprehensive rockburst monitoring method based on the MS technology, and the obtained evolutionary process of a rockburst were analyzed by numerical simulation, advanced three-dimensional numerical modeling and visualization can identify potentially hazardous areas and assist in planning and design underground structures [44–48]. Zhu et al. [49] proposed a numerical model capable of studying the dynamic failure process of rock under coupled static geo-stress and dynamic disturbance, and it is implemented into the rock failure process analysis (RFPA), a general finite element package to analyze the damage and failure process of engineering materials such as rock and concrete. Jia et al. [50] put forward a new energy index, the local energy release rate (LERR) to simulate the conditions causing rockburst. By tracking the peak and trough values of elastic strain energy intensity before and after brittle failure, the LERR was developed to help understand rockbursts from the viewpoint of energy release. As a problem encountered in engineering, no matter how the research direction and methods change, the prevention and control measures of rockbursts are undoubtedly the key things in the transformation of theory into practice. Dou et al. [51] presented the intensity weakening theory for rockbursts and a strong-soft-strong (3S) structural model for controlling the impact on rock surrounding roadways, with the objective of laying a theoretical foundation and establishing references for parameters for the weakening control of a rockburst. He et al. [52] pointed out that the “strong structure” must have the active high strength support and yielding function named “double strong” function, and the high-strength-yielding bolt can satisfy this requirement and so is regarded as an effective support form to prevent and resist the rockburst.

Currently, the prevention and control measures for rockbursts have made good achievements in engineering practice. However, owing to numerical simulation and theoretical analysis have always been effective ways in the field of rock mechanics, the main researches mainly focused on numerical model and calculation theory, but the detailed measures and field feedback effects are not directly involved. There are a few researches about the isolated measures for specific engineering applications, and no system has been formed. The relationship between different measures are still lacking in qualitative knowledge. Therefore, in this paper, a prevention and control system of a rockburst hazard based on active release and passive support is applied in the tunnel group of the Jinping II hydropower station in Sichuan Province, China. The mechanical principle of support during construction is analyzed. The active and passive measures are discussed in detail by field observation and numerical simulation of a rockburst. The results can provide a direct assist for the prevention and control of a rockburst in deep-buried underground engineering.

2. Project Overview

2.1. Geological Conditions

Jinping II Hydropower Station is located at Yalong River, Liangshan Prefecture, Sichuan Province, where the hydroelectric resources are very abundant, as shown in Figure 1a. It is a landmark project to implement the national strategy of “Western Development” and “West to East Power Transmission” and to promote a new leap forward in Sichuan’s economy. The station relies on the water flowing along the 150 km reach of Yalong River to generate electricity by using 310 m natural fall, as shown in Figure 1b. The total installed capacity is 4800 MW, and the annual average power generation can reach 24.23 TWh. In geology, the station is at the hilly area of the eastern Qinghai-Tibet Plateau, affected by the collision between the Eurasian plate and the Indian Ocean plate. In the deep hole drilling of this engineering, the phenomenon of rock cakes is found, which is unique in high geostress environment, and obviously shows an increase with burial depth. The engineering tunnel passes through hard rock strata such as marble, limestone and sandstone, and the strata from west to east is metamorphic medium to fine sandstone, lower Triassic (T_1) chlorite schist, marble of the Zagunao group, upper Triassic (T_3) marble, marble of the Baishan group (T_{2b}) and marble of the Yantang (T_{2y}) group. The bedding is parallel to the direction of the principal tectonic line and the faults all have a steep inclined angle, which can be divided into four structural groups in direction NNE (North-northeast), NNW (North-northwest), NE-NEE (Northeast- Northeasteast) and NW-NWW (Northwest-Northwestwest), respectively. The tensile and torsional joints are mainly in the NNE and approximately EW (East-west) direction, as shown in Figure 1c. The burial depths of tunnels are in 1500–2000 m, with a maximum depth reaching 2525 m. The measured maximum geostress is 80 MPa, the uniaxial compressive strength of marble in the engineering area is 60 to 120 MPa. Therefore, the strength–stress ratio of rock mass reaches 0.75 to 1.5, which has met the conditions for strong and even extremely strong rockburst.

In the construction of seven parallel tunnels of Jinping II Hydropower Station, the first one is the auxiliary tunnel A and B lines, then the drainage tunnel and four diversion tunnels are constructed. Auxiliary tunnels are constructed by drilling-blasting method, with an excavation diameter of 7.2 m and a gate-shaped excavation area of 45 m². The diversion tunnels are constructed by the tunnel boring machine (TBM) and the drilling-blasting method. The drilling-blasting part is adopted by the two-bench method, with a horseshoe-shaped section and an excavation diameter of 12.4 m. The excavation area of the upper bench is 110 m² and the lower bench is 60 m². The drainage tunnel is built between the auxiliary tunnel B and diversion tunnel 4 to discharge the gushing water safely and provide a transportation channel for the diversion tunnels. It is excavated with a full section TBM, with an excavation diameter of 7.2 m and a circular excavation area of 41 m².

2.2. Rockburst in Tunnels

Extremely strong rockburst occurred in the Jinping tunnels, and the slumping rock is hot and smoky. The typical lumpy and flaky rockburst in the construction site is shown in Figure 2, which lasts for a long time. This causes serious damage to the initial support and seriously hinders the construction. As shown in Figure 3a, the rockburst of the drainage tunnel resulted in the burying of TBM. The 80 mm steel plate of TBM was cut off by this extremely strong rockburst, and its main beam was damaged, as shown in Figure 3b. The advance of tunneling has been interrupted for a long time. It is estimated that the energy released by this rockburst is equivalent to the energy of the earthquake with magnitude 1.5, which shows how strong the degree of the rock burst is.

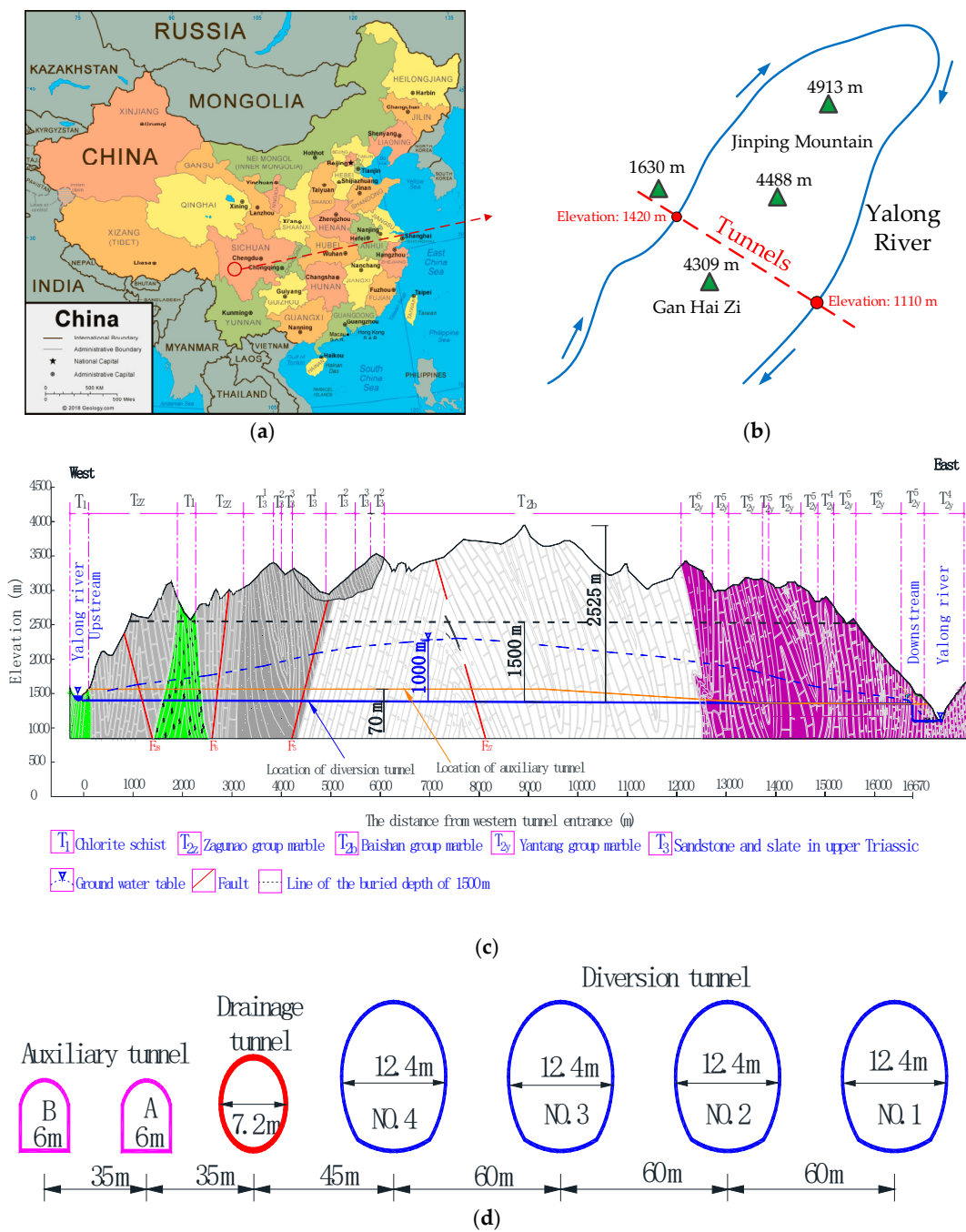


Figure 1. Deep tunnels of Jinping II hydropower station: (a) Map of China and location of the station; (b) plan of the station; (c) engineering geologic profile; and (d) layout and cross section of the tunnels.



Figure 2. Rockburst in auxiliary tunnels: (a) Extremely strong rockburst; (b) induced collapse and (c) support structure damage.



Figure 3. Rockburst in drainage tunnel: (a) Tunnel boring machine (TBM) is buried and (b) 80 mm steel plate is damaged.

Therefore, in order to ensure the safety of construction personnel and equipment, and make the follow-up construction advance smoothly, it is urgent to take effective measures to prevent and control the rockburst, especially extremely strong rockburst.

3. Numerical Simulation

What is different from the normal geotechnical engineering materials like soil and concrete is that there are many discontinuities in natural surrounding rock, such as faults, joints and layers. These discontinuities play a dominant role in the mechanical behavior of surrounding rock under static and dynamic loads. The discrete element method is especially suitable for simulating discontinuous medium problems, and it regards surrounding rock as being composed of discrete rock blocks and joint planes between them. Rock blocks can move, deform and rotate, while joint surfaces can be compressed, slid and separated, so that surrounding rock can be simulated better.

Based on discrete element software 3DEC, considering the initial geostress field before excavation and stress redistribution after excavation and spatiotemporal effect of support, this paper taking the auxiliary tunnels, which are first constructed and faced with serious rockburst hazards as an example, discussed the mechanism and simulation results of several measures, which can provide a theoretical basis to establish a reasonable technical scheme for rockburst prevention and control under high geostress conditions.

3.1. Model Description

In order to avoid the influence of the boundary effect on the calculation results, the size of the numerical model was set to the horizontal direction $x = -70$ to 70 m, longitudinal $y = -60$ to 60 m and vertical $z = -40$ to 40 m, respectively. The initial geostress was simulated based on the buried depth and fixed displacement method. As shown in Figure 4, the normal displacement constraints were applied to the edges of the model. Based on the strength test of the surrounding rock and the field geological

survey data, the mechanical parameters of model were determined in Table 1. Mohr-Coulomb yield criterion was adopted for surrounding rock and support, that was the possible failure of the rock and support were considered in the calculation process.

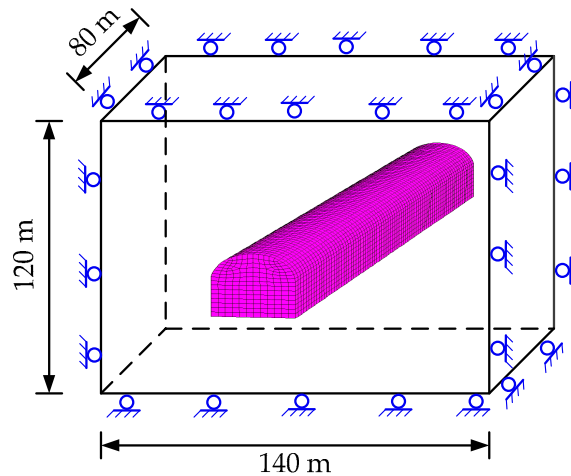


Figure 4. Three-dimensional numerical model.

Table 1. Mechanical parameters of surrounding rock.

Density ρ (kg/m ³)	Poisson Ratio μ	Internal Friction Angle φ (°)	Cohesion C (MPa)	Elasticity Modulus E (GPa)	Lateral Pressure Coefficient
2840	0.25	45	7.5	80	0.8

Surface water spraying and borehole water injection in surrounding rock are common methods for rock soften. However, the effect of these methods is closely related to the water absorption of surrounding rock. The surrounding rock of Jinping tunnels is mainly marble, which has a water absorption of less than 0.1%. There was a very limited role to play through surface water spraying and borehole water injection in surrounding rock in this project, therefore, it was not necessary to do more research. Based on the phenomenon of rockburst in auxiliary tunnels, it had the characteristics of fracture induction and dynamic impact damage, and this kind of rockburst had the uncertainty of the dynamic source (microseismic source) and damage location. It is advisable to take measures to release the energy of the microseismic source and make the high stress transfer to the deeper surrounding rock. In the strong rockburst area, this transfer could be achieved by active measures like stress release hole and advanced stress relief blasting.

3.2. Stress Release Hole

Boring holes in the tunnel wall after excavation, the tangential stress of surrounding rock can be released through the deformation of holes, which is a common method of rock burst control. The effect of this method is closely related to the size, length and longitudinal spacing of boreholes, which will be discussed in the simulation of this section, shown in Figure 5. The stress release rate is used to simulate the three-dimensional space effect of boreholes. In order to analyze the effect of various parameters on rockburst prevention, eight conditions were designed as shown in Table 2.

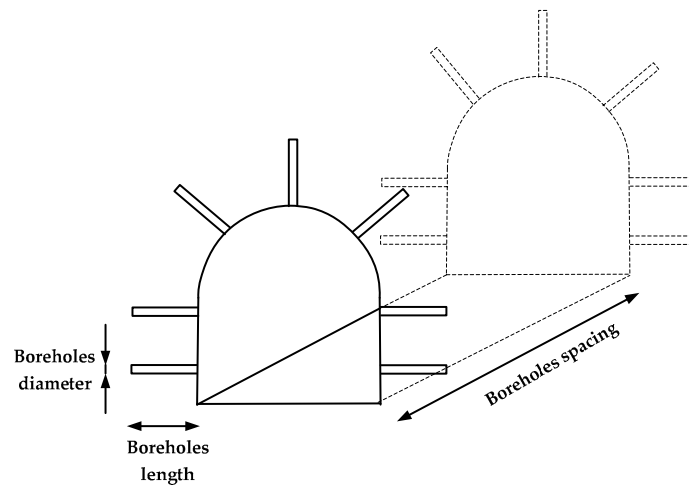


Figure 5. Arrangement of boreholes.

Table 2. Parameters of simulated conditions.

Conditions Number	Boreholes Diameter (mm)	Boreholes Length (m)	Boreholes Spacing (m)
1	50	2	2
2	100	2	2
3	150	2	2
4	200	2	2
5	100	1	2
6	100	3	2
7	100	2	1
8	100	2	3

Taking the No. 3 condition as an example, the typical displacement distribution of surrounding rock after boring holes is shown in Figure 6. The convergence of holes induced the radial deformation of tunnel turns to tangential deformation around the boreholes. Figure 7 shows the distribution of maximum principal stress in surrounding rock before and after boring holes. After boring holes, the maximum principal stress of tunnel wall was reduced about 12%. That is, the stress of surrounding rock was released after boring, which could reduce the risk of rockburst.

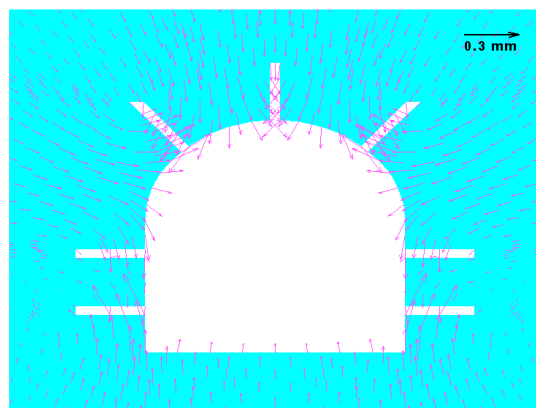


Figure 6. Displacement distribution of surrounding rock.

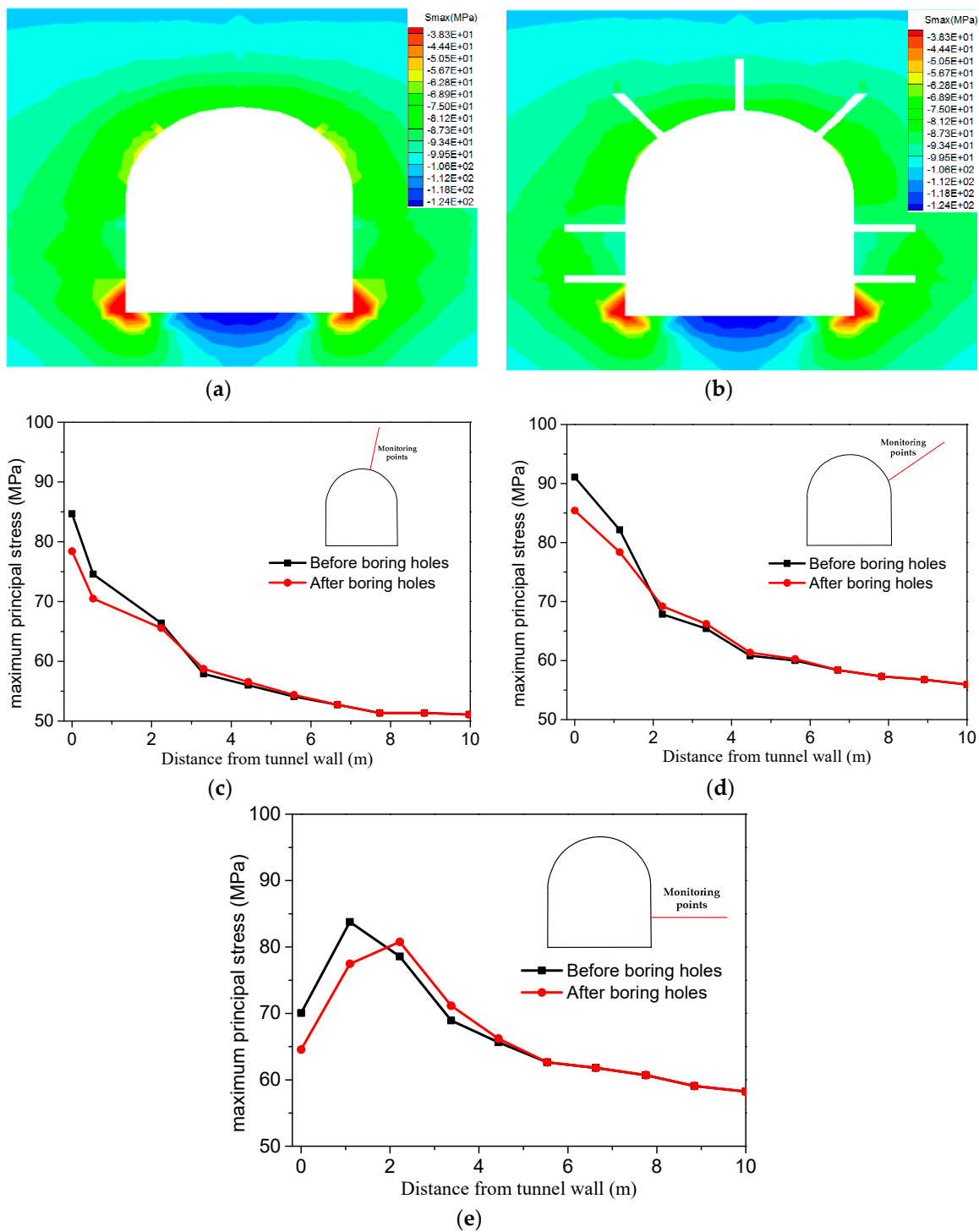


Figure 7. The change of maximum principal stress in surrounding rock at different locations: (a) Before boring holes; (b) after boring holes; (c) curves at the vault; (d) curves at the spandrel and (e) curves at the sidewall.

Figure 8 shows the effect of boreholes diameter on stress release rate. The stress release rate of surrounding rock increased linearly with the diameter of borehole. At the same time, the stress decreased in the range of 2 m around the tunnel wall, but the stress increased in the internal rock mass. It also proved that transferring the stress in the surrounding rock to the internal rock was the mechanism of the boreholes stress release method, and the surface rock wall with relatively low stress acted as a protective barrier.

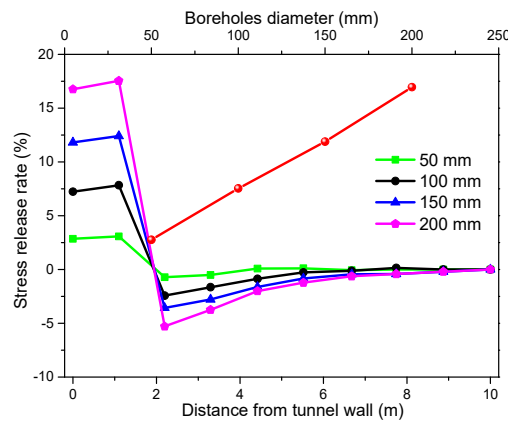


Figure 8. The effect of boreholes diameter on stress release rate.

As we could see from the Figure 9, the longer the drill hole length, the larger the stress release range, but the stress release rate of the tunnel wall did not increase significantly, which shows that increasing the boreholes length had little effect on rockburst prevention. The smaller the borehole spacing, the greater the stress release rate, which is in accordance with the general experience. However, as the spacing continues to decrease, the growth rate of stress release rate gradually slows down, which needs to be weighed based on the workload of boring.

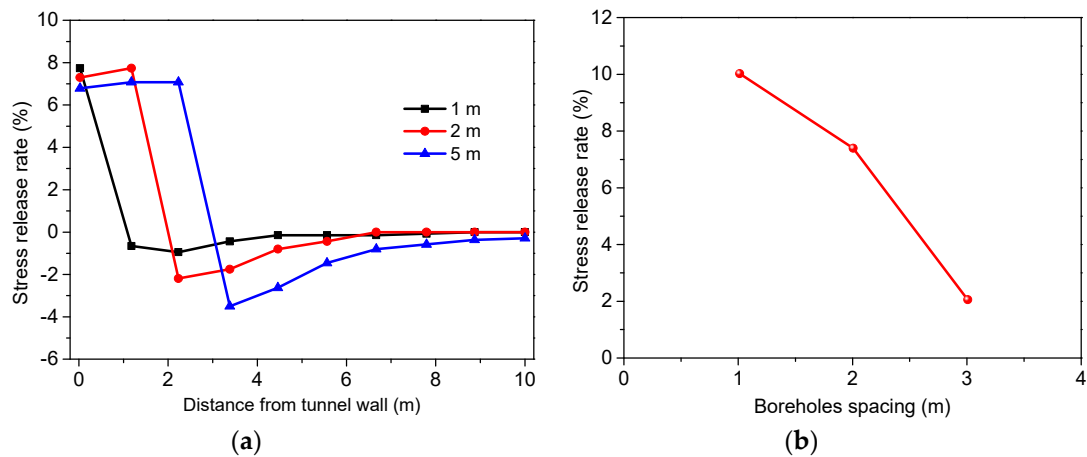


Figure 9. The effect of boreholes on stress release rate: (a) Boreholes length and (b) boreholes spacing.

3.3. Advanced Stress Relief Blasting

From the above Section 3.2, the release rate of stress release hole was under 20%. However, under the conditions of strong rockburst, even extremely strong rockburst, this method can no longer meet the requirements of rockburst control. At this point, advanced stress relief blasting is a better choice, which can generate cracks to decrease the integrity and energy accumulation ability of rock mass through setting blasting in high of stress zone of internal rock. In this way, the accumulated energy can be relieved, and the harm of rockburst can be weakened or even eliminated. The angle between advanced oblique holes and tunnel axis is θ , and blasting creates a fractured zone with thickness δ in the surrounding rock, which are shown in Figure 10. The surface rock wall with thickness h can act as a protective barrier.

In this simulation, let $\theta = 25^\circ$, $h = 2$ m and $\delta = 1$ m, the change of the maximum principal stress in surrounding rock before and after blasting is shown in Figure 11. After blasting, a distinct stress release zone was formed, the maximum principal stress of tunnel sidewall was reduced from 63 MPa to 43 MPa, and the release rate reached about 33%, which was about twice as the stress release hole method. However, because of the small section of the auxiliary tunnel, the operation of the working

machinery was stiff. What is more, the loosening circle of surrounding rock after blasting was large under high geostress. In order to ensure the safe distance of fractured zone and the enough thickness of protective rock wall, blasting holes need to be very deep, which takes a lot of time. Therefore, a new 14-hole advanced stress relief blasting scheme was proposed, shown in Figure 12, which was composed of main shallow holes on the tunnel face and supplementary deep holes on the periphery.

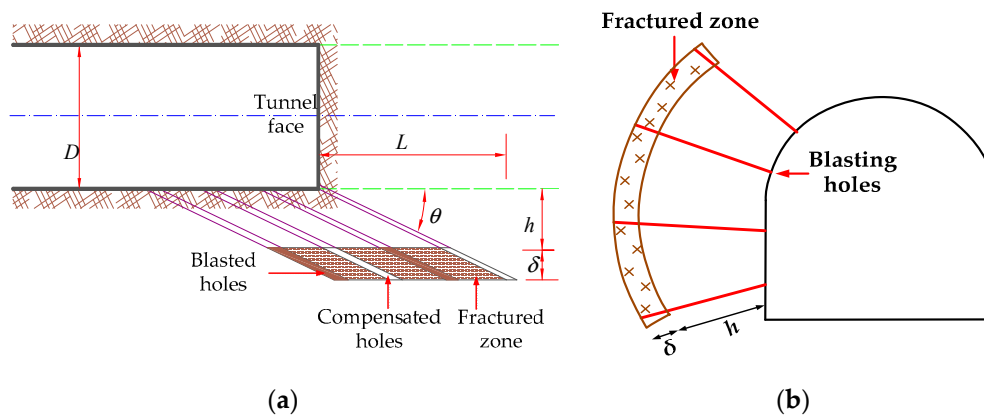


Figure 10. The diagram of advanced oblique holes and fractured zone: (a) Top view and (b) elevation view.

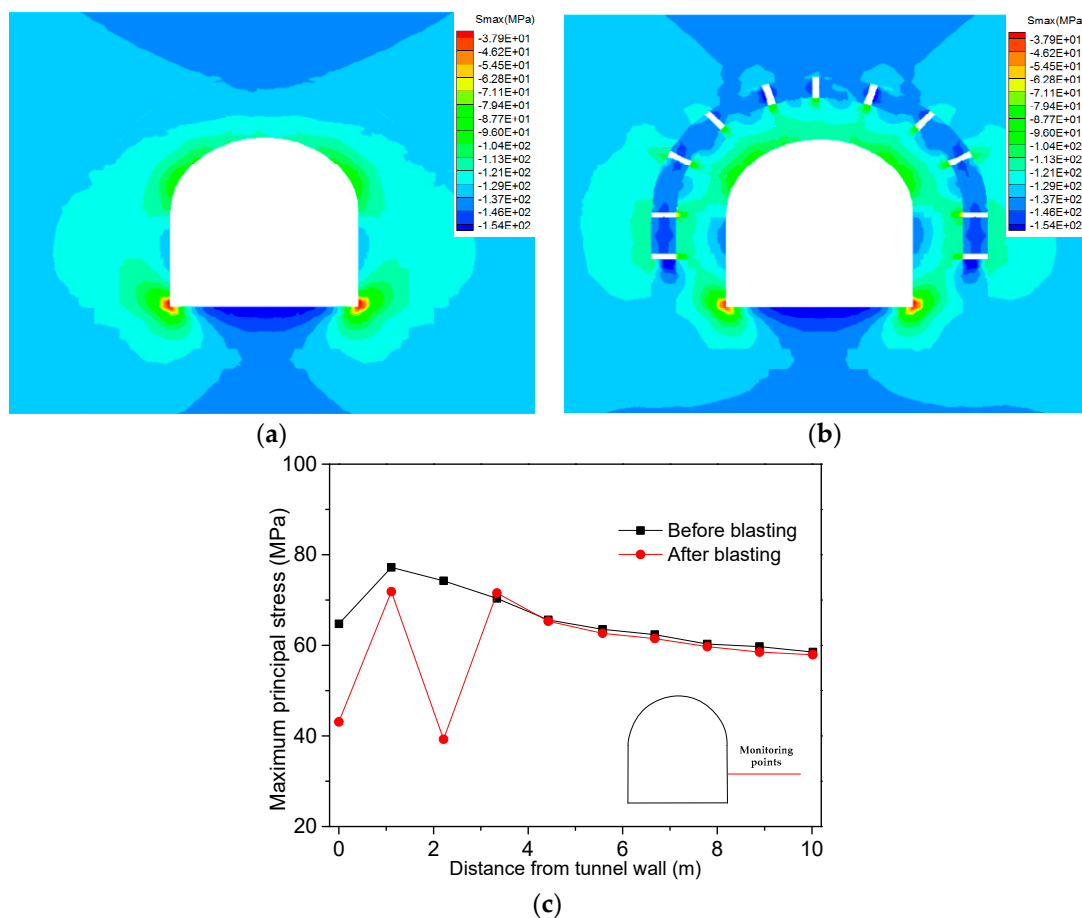


Figure 11. The change of maximum principal stress in surrounding rock before and after blasting: (a) Before blasting; (b) after blasting and (c) at the sidewall.

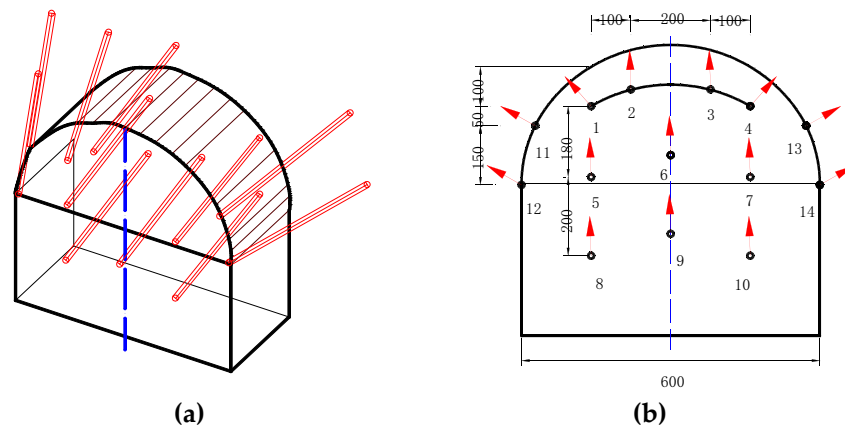


Figure 12. 14-hole advanced stress relief blasting scheme: (a) Side view and (b) elevation view (mm).

3.4. Rapid Combined Support

Different from active measures that stress release hole and advanced stress relief blasting relieving and transferring the stress of surrounding rock, rapid combined support is also a passive way to prevent and control the rockburst under high geostress. Rockburst is prevented through providing radial support stress to rock, controlling the deformation of rock, improving the stress condition of rock and reducing the break of rock. Meanwhile, the harm of a rockburst is controlled by shortening support operation time, increasing support early strength. In this simulation, the same anchor and different thickness (0.05 m, 0.1 m, 0.2 m, 0.5 m, 1.0 m and 1.5 m) of shotcrete was adopted to study on the failure range of surrounding rock and the failure state of shotcrete. The support parameters are shown in Tables 3 and 4.

Table 3. The parameters of anchor.

Density (kg/m ³)	Diameter (mm)	Elasticity Modulus (GPa)	The Tensile/Pressure Strength (tons)	Length (m)	Spacing (m)
7500	22	210	25	3.0	2.0

Table 4. The parameters of shotcrete.

Density (kg/m ³)	Thickness (m)	Elasticity Modulus (GPa)	The Tensile/Pressure Strength (MPa)	Residual Tensile Strength (MPa)	Poisson Ratio
2500	0.05–1.5	21	3.0/30.0	1.0	0.15

Distribution of the plastic zone in surrounding rock with different thickness of shotcrete is shown in Figure 13. With the increase of shotcrete thickness, the plastic zone in the surrounding rock of the sidewall and vault decreased gradually, while the plastic zone in the surrounding rock of the bottom changed little. Support could improve the stress condition of surrounding rock, and the thicker the shotcrete is, the better the effect is. As we can see from Figure 14, increasing the thickness of shotcrete could reduce the damage zone of shotcrete itself, effectively controlling the occurrence of a rockburst.

Based on the existing engineering experience and the simulation results in this section, we know that the timely construction of high-strength support structure was an important part of rockburst prevention and control. In order to achieve that better, this paper introduced two measures: Water swelling anchor and nano-admixture shotcrete.

3.4.1. Water Swelling Anchor

Water swelling anchor is also called the Swellex anchor, consisting of a steel tubular anchor, mechanical installation arm and pneumatic high-pressure water pump, shown in Figure 15. During the anchor installation process, when the water pressure in the anchor reaches the limit, the high-pressure

water pump stops working automatically. A good connection is once formed between the anchor and the rock mass, then the installation process is completed immediately.

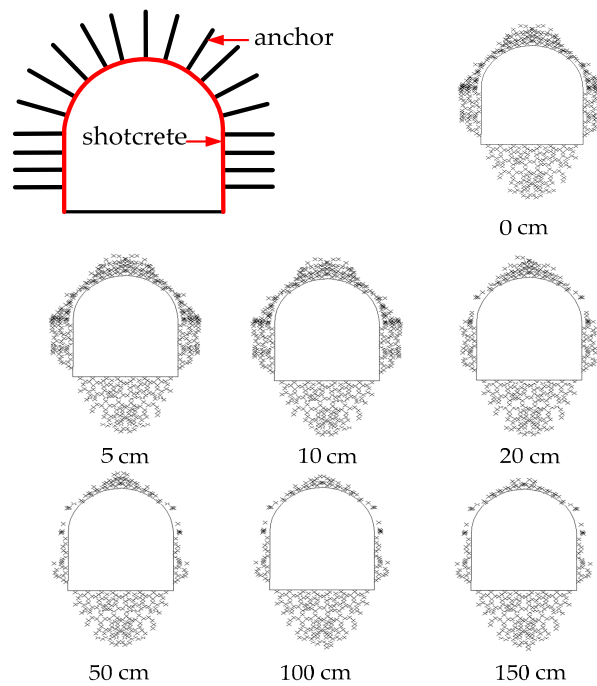


Figure 13. Plastic zone in surrounding rock with different shotcrete thickness.

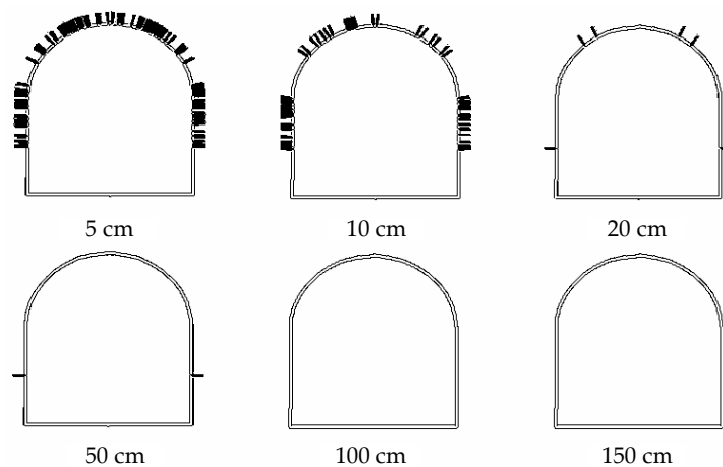


Figure 14. Damage zone of shotcrete with different shotcrete thickness.

Compared with normal anchors, water swelling anchors have the following characteristics. Water swelling anchors can be carried out by manual, semi-mechanized or fully mechanized methods, which is handier, with higher quality and easier to master. What is more significant is that the installation speed of water swelling anchors is five times higher than normal ones, and the average installation time of one anchor is only 2–3 min. It can adapt to various stratum conditions from sand, clay to the hardest granite, and its bearing capacity is not affected by the surrounding rock joints, but the anchorage strength increases when the joints deform. However, water swelling anchors also have some defects. Although the installation cost is low, this anchor is more expensive. The water swelling anchor is short of corrosion resistance and can only be used as a temporary support in the water environment. In order to ensure long-term stability of surrounding rock, mortar anchors should be supplemented into the anchor system, and the supplement account for 50% of the total is recommended.

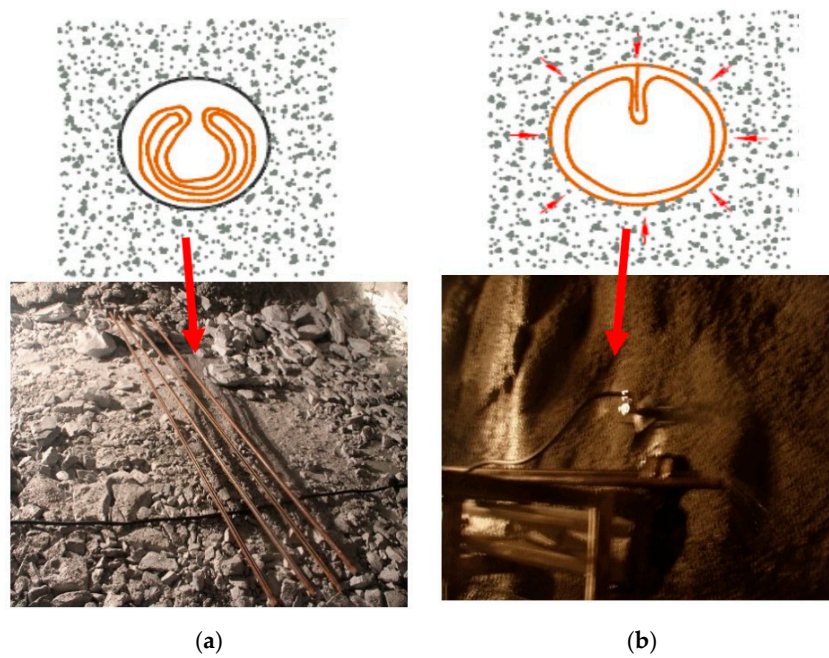


Figure 15. Water swelling anchor: (a) Samples and (b) pressurization.

3.4.2. Nano-Admixture Shotcrete

Shotcrete in rockburst area needs fast setting speed, high early strength and thick primary shotcrete thickness. In order to achieve this, a new material was added into shotcrete, which is a nano-admixture made of zeolite by mechanical grinding and had the functions of water reducing, early setting and strengthening.

The optimum content of admixture is 6–8% of the total weight. The nano-admixture shotcrete has a thickness of 30–50 cm at one time and final setting within 2 min. Its strength can reach 1 MPa in 2 h while normal shotcrete can reach this strength in about 10 h. The bonding force of this shotcrete is more than 7–8 times that of the normal concrete. What is more, the water reduction rate is 30%, the bleeding ratio is less than 17%, and the fluidity is improved, which can effectively improve the cohesion and water retention of concrete mixtures, and the slump loss rate is less than 12%, and the rebound rate is less than 10%. Due to the excellent performance of optimized shotcrete, also considering that the quality of molding concrete in composite lining is hard to guarantee and it takes a long time to operate, the secondary nano-admixture concrete is used to replace the original molding lining, and the steel mesh and steel arch ribs are used together. The combined support is shown in Figure 16.

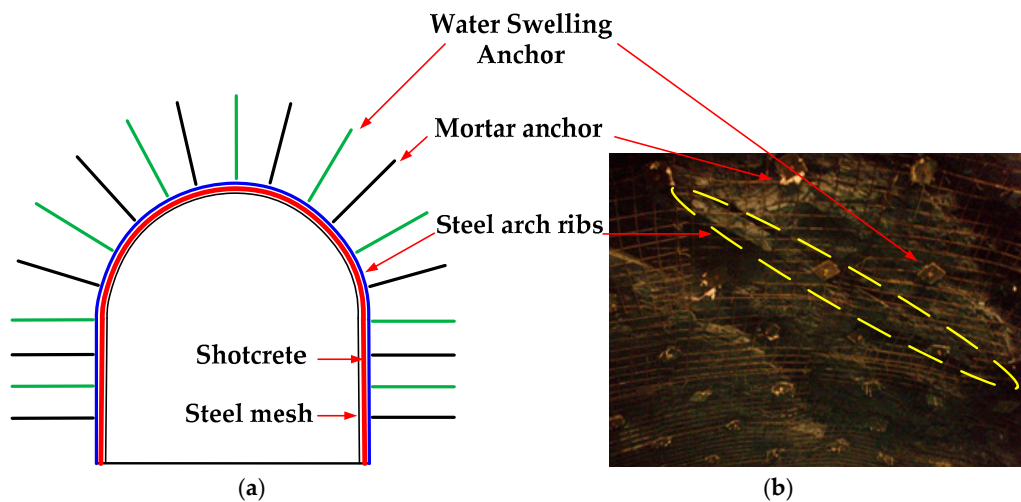


Figure 16. Combined rapid support: (a) Cross section diagram and (b) steel mesh and steel arch ribs.

4. Field Application of Research Results

Based on the research of rockbursts in auxiliary tunnels, the prevent and control system combining stress release methods and rapid support methods have been applied in the reconstruction of auxiliary tunnels and new-construction diversion tunnels, where the rockburst may be even more serious. Initially, the length of the rockburst section in auxiliary tunnels reached 3101 m, about 9.9% of the total excavation length. After applying these measures to remedy in auxiliary tunnels, the rockburst phenomenon has obviously weakened or even completely disappeared. What is more, a rockburst basically does not occur in diversion tunnels where systematic measures are taken. The systematic steps and good effects are shown in the Figure 17.

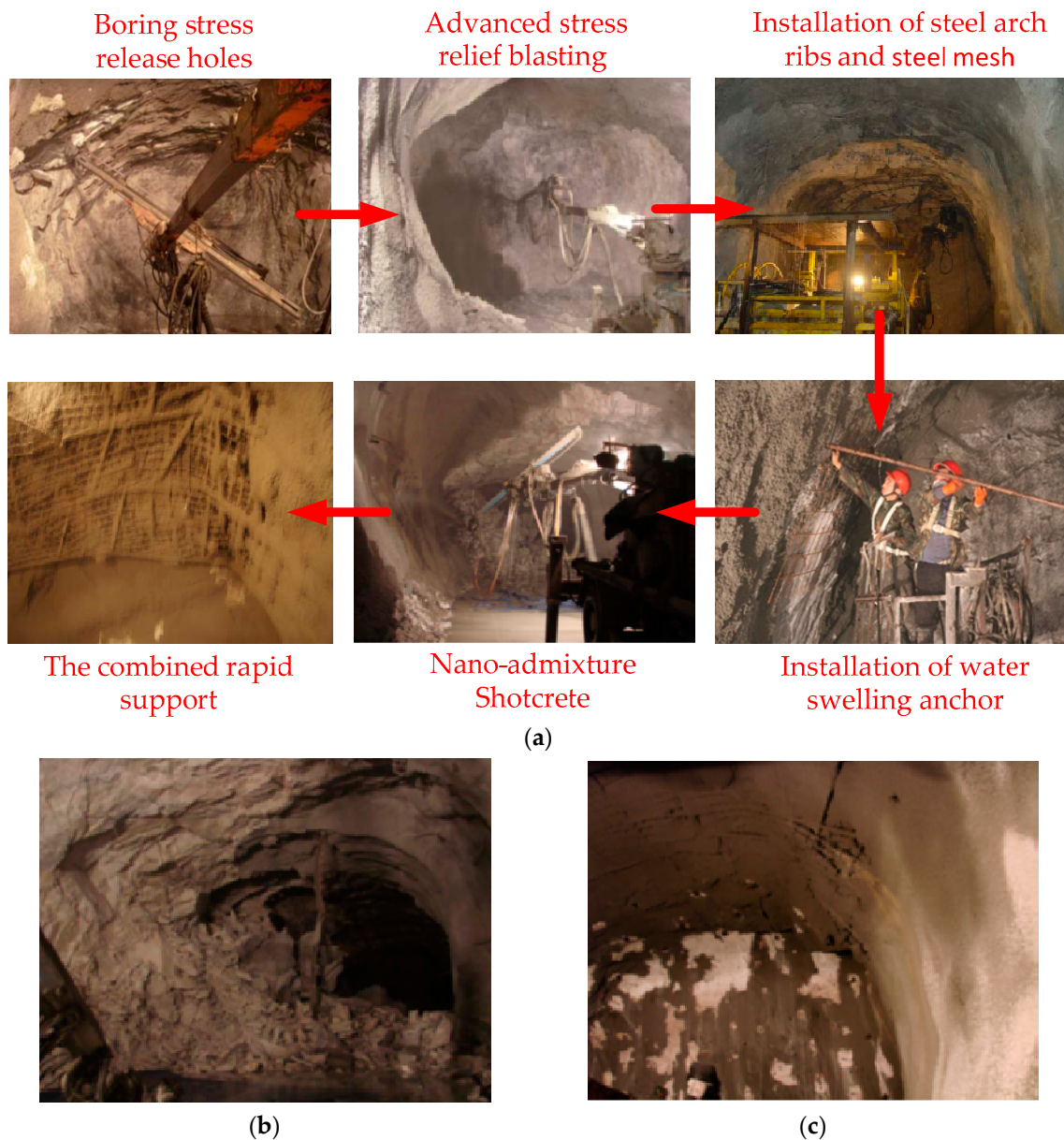


Figure 17. Field application in diversion tunnels: (a) Application steps; (b) before application and (c) after application.

5. Conclusions

Rockburst hazards induced by high geostress are particularly prominent in underground engineering construction. Prevention and control of rockburst is still a global challenge in the field of geotechnical engineering, which is of great significance. Based on the tunnels of the Jinping II hydropower station in China, this paper analyzed the mechanical principle of support in the construction process, and discussed the active release and passive support by numerical simulation and field application in detail. The following conclusions were drawn:

The surrounding rock of auxiliary tunnel is mainly marble with poor water absorption, the effect of common measures like surface water spraying and borehole water injection is very little. Boring holes in tunnel wall can release the energy of the microseismic source and transfer the high stress to the deeper surrounding rock, and the surface rock wall with relatively low stress acts as a protective barrier. The stress release rate of surrounding rock increases linearly with the diameter of borehole. The smaller the borehole spacing, the greater the stress release rate. However, increasing the boreholes length has little effect on rockburst prevention. In this project, with holes diameter of 150 mm and length of 2 m and spacing of 2 m, the stress release rate was about 12%.

Advanced stress relief blasting can also release the energy and transfer stress to the deeper surrounding rock and form a protective rock wall. Comparing to the stress release hole, advanced stress relief blasting reaches is more useful for stronger rockburst conditions, which reaches about 33% stress release rate. It can also make the surface rock wall with relatively low stress act as a protective barrier. Considering the limit of tunnel small section and longtime needed for boring holes, a new 14-hole advanced stress relief blasting scheme was proposed, which was composed of main shallow holes on the tunnel face and supplementary deep holes on the periphery.

Different from active measures that stress release hole and advanced stress relief blasting releasing and transferring the stress of surrounding rock, passive measures are also an effective way to prevent and control the rockburst under high geostress. Based on the simulation of tunnel with different thickness of shotcrete, it could be found that high-strength rapid support could reduce the damage zone of shotcrete itself, effectively control the occurrence of rockburst. In order to achieve that better, this paper introduced two measures: Water swelling anchor and nano-admixture shotcrete. The installation speed of water swelling anchors is five times higher than normal ones, but because of low corrosion resistance it needs to cooperate with mortar bolts. The nano-admixture shotcrete has high early strength, high one-time shotcrete thickness and other excellent characteristics. The combined support composed of swelling anchor, nano-admixture shotcrete, steel mesh and steel arch ribs were proposed, which achieves good effect in practice.

Author Contributions: H.Z. analyzed the calculation results and wrote the article; Y.Z. carried out the calculations; L.C. provided the information of the parameters; W.H. processed the data; S.C. offered useful suggestions for the preparation and writing of the paper.

Funding: The study was supported by Sichuan Science and Technology Program (No. 2019YFG0460) and the National Natural Science Foundation of China (NSFC) under Grant No. 51508037.

Acknowledgments: We also highly appreciate the contribution of data collection from 2nd Engineering Pte Ltd. of the Chinese Railway 2nd Bureau, Ertan Hydropower Development Company, Ltd., and East China Investigation and Design Institution. Finally, the authors would like to thank reviewers for useful comments and editors for improving the manuscript.

Conflicts of Interest: The authors declare no conflict of interest.

References

1. Zhang, H.; Chen, L.; Zhu, Y.; Zhou, Z.; Chen, S. Stress Field Distribution and Deformation Law of Large Deformation Tunnel Excavation in Soft Rock Mass. *Appl. Sci.* **2019**, *9*, 865. [[CrossRef](#)]
2. Zhang, Z.Q.; Zhang, H.; Tan, Y.J.; Yang, H.Y. Natural wind utilization in the vertical shaft of a super-long highway tunnel and its energy saving effect. *Build. Environ.* **2018**, *145*, 140–152. [[CrossRef](#)]
3. Zhu, Y.; Chen, L.; Zhang, H.; Zhou, Z.; Chen, S. Physical and Mechanical Characteristics of Soft Rock Tunnel and the Effect of Excavation on Supporting Structure. *Appl. Sci.* **2019**, *9*, 1517. [[CrossRef](#)]
4. Tang, F.; Li, L.J.; Dong, M.S.; Wang, Q.; Mei, F.Z.; Hu, L.H. Characterization of buoyant flow stratification behaviors by Richardson (Froude) number in a tunnel fire with complex combination of longitudinal ventilation and ceiling extraction. *Appl. Therm. Eng.* **2017**, *110*, 1021–1028. [[CrossRef](#)]
5. Kaiser, P.K.; Cai, M. Design of rock support system under rockburst condition. *J. Rock Mech. Geotech. Eng.* **2012**, *4*, 215–227. [[CrossRef](#)]
6. Mei, F.Z.; Tang, F.; Ling, X.; Yu, J.S. Evolution characteristics of fire smoke layer thickness in a mechanical ventilation tunnel with multiple point extraction. *Appl. Therm. Eng.* **2017**, *111*, 248–256. [[CrossRef](#)]
7. Wang, F.; Wang, M.N.; Huo, J.X. The effects of the passive fire protection layer on the behavior of concrete tunnel linings: A field fire testing study. *Tunn. Undergr. Sp. Tech.* **2017**, *69*, 162–170. [[CrossRef](#)]
8. Tang, F.; Cao, Z.L.; Adriana, P.; Wang, Q. A study on the maximum temperature of ceiling jet induced by rectangular-source fires in a tunnel using ceiling smoke extraction. *Int. J. Therm. Sci.* **2018**, *127*, 329–334. [[CrossRef](#)]
9. Wang, F.; Wang, M.N.; Ricky, C.; Wang, Y. Numerical study on fire smoke movement and control in curved road tunnels. *Tunn. Undergr. Sp. Tech.* **2017**, *67*, 1–7. [[CrossRef](#)]
10. Wang, F.; Wang, M.N. A computational study on effects of fire location on smoke movement in a road tunnel. *Tunn. Undergr. Sp. Tech.* **2016**, *51*, 405–413. [[CrossRef](#)]
11. Zhang, Z.; Li, H.; Yang, H.; Wang, B. Failure modes and face instability of shallow tunnels under soft grounds. *Int. J. Damage Mech.* **2019**, *28*, 566–589. [[CrossRef](#)]
12. Wang, F.; Luo, F.Y.; Huang, Y.B.; Zhu, L.; Hu, H. Thermal analysis and air temperature prediction in TBM construction tunnels. *Appl. Therm. Eng.* **2019**, *158*, 113822. [[CrossRef](#)]
13. Basson, F.R.P.; Van Der Merwe, S. Seismicity Management at Hill 50 Gold Mine, Western Australia. In Proceedings of the Fourth International Seminar on Deep and High Stress Mining, Perth, Australia, 7–9 November 2007; Australian Centre for Geomechanics: Crawley, Perth, WA, Australia, 2007; pp. 233–242.
14. Urbancic, T.I.; Trifu, C.I. Recent advances in seismic monitoring technology at Canadian mines. *J. Appl. Geophys.* **2000**, *45*, 225–237. [[CrossRef](#)]
15. Durrheim, R.J.; Haile, A.; Roberts, M.K.C.; Schweitzer, J.K.; Spottiswoode, S.M.; Klokow, J.W. Violent failure of a remnant in a deep South African gold mine. *Tectonophysics* **1998**, *289*, 105–116. [[CrossRef](#)]
16. Milev, A.M.; Spottiswoode, S.M.; Rorke, A.J.; Finnie, G.J. Seismic monitoring of a simulated rockburst on a wall of an underground tunnel. *J. S. Afr. Inst. Min. Metall.* **2001**, *101*, 253–260.
17. Feng, X.T.; Yang, Y.; Feng, G.L.; Xiao, Y.X.; Chen, B.R.; Jiang, Q. Fractal behaviour of the microseismic energy associated with immediate rockbursts in deep, hard rock tunnels. *Tunn. Undergr. Space Technol.* **2016**, *51*, 98–107. [[CrossRef](#)]
18. Zhang, H.; Chen, L.; Chen, S.G.; Sun, J.C.; Yang, J.S. The spatiotemporal distribution law of microseismic events and rockburst characteristics of the deeply buried tunnel group. *Energies* **2018**, *11*, 3257. [[CrossRef](#)]
19. Zhang, Z.Q.; Shi, X.Q.; Wang, B.; Li, H.Y. Stability of NATM tunnel faces in soft surrounding rocks. *Comput. Geotech.* **2018**, *96*, 90–102. [[CrossRef](#)]
20. Blake, W.; Hedley, D.G.F. *Rockbursts, Case Studies from North American Hardrock Mines*; Society for Mining, Metallurgy, and Exploration: Littleton, CO, USA, 2003.
21. Ortlepp, W.D.; Stacey, T.R. Rockburst mechanisms in tunnels and shafts. *Tunn. Undergr. Space Technol.* **1994**, *9*, 59–65. [[CrossRef](#)]
22. Martin, C.D.; Kaiser, P.K.; McCreath, D.R. Hoek-Brown parameters for predicting the depth of brittle failure around tunnels. *Can. Geotech. J.* **1999**, *36*, 136–151. [[CrossRef](#)]
23. Beck, D.A.; Brady, B.H.G. Evaluation and application of controlling parameters for seismic events in hard-rock mines. *Int. J. Rock Mech. Min. Sci.* **2002**, *39*, 633–642. [[CrossRef](#)]

24. Li, T.B.; Ma, C.C.; Zhu, M.L.; Meng, L.B.; Chen, G.Q. Geomechanical types and mechanical analyses of rockbursts. *Eng. Geol.* **2017**, *222*, 72–83. [[CrossRef](#)]
25. Hatzor, Y.H.; He, B.G.; Feng, X.T. Scaling rockburst hazard using the DDA and GSI methods. *Tunn. Undergr. Space Technol.* **2017**, *70*, 343–362. [[CrossRef](#)]
26. Chen, B.R.; Feng, X.T.; Li, Q.P.; Luo, R.Z.; Li, S.J. Rock burst intensity classification based on the radiated energy with damage intensity at Jinping II hydropower station, China. *Rock Mech. Rock Eng.* **2015**, *48*, 289–303. [[CrossRef](#)]
27. Ma, K.; Tang, C.A.; Wang, L.X.; Tang, D.H.; Zhuang, D.Y.; Zhang, Q.B.; Zhao, J. Stability analysis of underground oil storage caverns by an integrated numerical and microseismic monitoring approach. *Tunn. Undergr. Space Technol.* **2016**, *54*, 81–91. [[CrossRef](#)]
28. Xie, H.; Pariseau, W.G. Fractal character and mechanism of rock bursts. *Int. J. Rock Mech. Min. Sci.* **1993**, *30*, 343–350. [[CrossRef](#)]
29. Gong, Q.M.; Yin, L.J.; Wu, S.Y.; Zhao, J.; Ting, Y. Rock burst and slabbing failure and its influence on TBM excavation at headrace tunnels in Jinping II hydropower station. *Eng. Geol.* **2012**, *124*, 98–108. [[CrossRef](#)]
30. He, M.C.; Sousa, L.R.; Miranda, T.; Zhu, G.L. Rockburst laboratory tests database—Application of data mining techniques. *Eng. Geol.* **2015**, *185*, 116–130. [[CrossRef](#)]
31. Müller, W. Numerical simulation of rock bursts. *Min. Sci. Technol.* **1991**, *12*, 27–42. [[CrossRef](#)]
32. Hedley, D.G.F. *Rockburst Handbook for Ontario Hardrock Mines*; Canada Centre for Mineral and Energy Technology, Mining Research Laboratories (CANMET): Ottawa, ON, Canada, 1992.
33. Kaiser, P.K.; MacCreath, D.R.; Tannant, D.D. *Canadian Rockburst Support Handbook: Prepared for Sponsors of the Canadian Rockburst Research Program 1990–1995*; Geomechanics Research Centre: Sudbury, ON, Canada, 1996.
34. Stacey, T.R. Dynamic rock failure and its containment—A Gordian knot design problem. In Proceedings of the First International Conference on Rock Dynamics and Applications (RocDyn 1), Lausanne, Switzerland, 6–8 June 2013; Swit State of the Art. CRC Press: Balkema, Switzerland, 2013.
35. Linkov, A.V. Dynamic Phenomena in Mines and the Problem of Stability. Ph.D. Thesis, University of Minnesota, Minneapolis, MN, USA, 1992.
36. Yang, C.X.; Luo, Z.Q.; Hu, G.B.; Liu, X.M. Application of a microseismic monitoring system in deep mining. *J. Univ. Sci. Technol. Beijing* **2007**, *14*, 6–8. [[CrossRef](#)]
37. Wang, J.M.; Zeng, X.H.; Zhou, J.F. Practices on rockburst prevention and control in headrace tunnels of Jinping II hydropower station. *J. Rock Mech. Geotech. Eng.* **2012**, *4*, 258–268. [[CrossRef](#)]
38. Wang, H.L.; Ge, M.C. Acoustic emission/microseismic source location analysis for a limestone mine exhibiting high horizontal stresses. *Int. J. Rock Mech. Min. Sci.* **2008**, *45*, 720–728. [[CrossRef](#)]
39. Afraei, S.; Shahriar, K.; Madani, S.H. Developing intelligent classification models for rock burst prediction after recognizing significant predictor variables, Section 1: Literature review and data preprocessing procedure. *Tunn. Undergr. Space Technol.* **2019**, *83*, 324–353. [[CrossRef](#)]
40. Cai, W.; Dou, L.M.; Zhang, M.; Cao, W.Z.; Shi, J.Q.; Feng, L.F. A fuzzy comprehensive evaluation methodology for rock burst forecasting using microseismic monitoring. *Tunn. Undergr. Space Technol.* **2018**, *80*, 232–245. [[CrossRef](#)]
41. Xu, J.; Jiang, J.D.; Xu, N.; Liu, Q.S.; Gao, Y.F. A new energy index for evaluating the tendency of rockburst and its engineering application. *Eng. Geol.* **2017**, *230*, 46–54. [[CrossRef](#)]
42. Srinivasan, C.; Arora, S.K.; Benady, S. Precursory monitoring of impending rockbursts in Kolar gold mines from microseismic emissions at deeper levels. *Int. J. Rock Mech. Min. Sci.* **1999**, *36*, 941–948. [[CrossRef](#)]
43. Li, S.J.; Feng, X.T.; Li, Z.H.; Chen, B.R.; Zhang, C.Q.; Zhou, H. In situ monitoring of rockburst nucleation and evolution in the deeply buried tunnels of Jinping II hydropower station. *Eng. Geol.* **2012**, *137*, 85–96. [[CrossRef](#)]
44. Huang, R.Q.; Wang, X.N. Analysis of dynamic disturbance on rock burst. *Bull. Eng. Geol. Environ.* **1999**, *57*, 281–284. [[CrossRef](#)]
45. Amin, M.; Ming, C. Numerical modeling of rockburst near fault zones in deep tunnels. *Tunn. Undergr. Space Technol.* **2018**, *80*, 164–180.
46. Li, X.; Li, X.F.; Zhang, Q.B.; Zhao, J. A numerical study of spalling and related rockburst under dynamic disturbance using a particle-based numerical manifold method (PNMM). *Tunn. Undergr. Space Technol.* **2018**, *81*, 438–449. [[CrossRef](#)]

47. Weng, L.; Huang, L.Q.; Taheri, A.; Li, X.B. Rockburst characteristics and numerical simulation based on a strain energy density index: A case study of a roadway in Linglong gold mine, China. *Tunn. Undergr. Space Technol.* **2017**, *69*, 223–232. [[CrossRef](#)]
48. Hu, L.H.; Ma, K.; Liang, X.; Tang, C.; Wang, Z.W.; Yan, L.B. Experimental and numerical study on rockburst triggered by tangential weak cyclic dynamic disturbance under true triaxial conditions. *Tunn. Undergr. Space Technol.* **2018**, *81*, 602–618. [[CrossRef](#)]
49. Zhu, W.C.; Li, Z.H.; Zhu, L.; Tang, C.A. Numerical simulation on rockburst of underground opening triggered by dynamic disturbance. *Tunn. Undergr. Space Technol.* **2010**, *25*, 587–599. [[CrossRef](#)]
50. Jiang, Q.; Feng, X.T.; Xiang, T.B.; Su, G.S. Rockburst characteristics and numerical simulation based on a new energy index: A case study of a tunnel at 2,500 m depth. *Bull. Eng. Geol. Environ.* **2010**, *69*, 381–388. [[CrossRef](#)]
51. Dou, L.; Lu, C.; Mu, Z.; Gao, M.S. Prevention and forecasting of rock burst hazards in coal mines. *Min. Sci. Technol.* **2009**, *19*, 585–591. [[CrossRef](#)]
52. He, H.; Dou, L.M.; Gong, S.Y.; Wang, L.L.; Gao, M.S.; Zhang, X.F. Mechanism of rockburst prevention and supporting control technology in roadways. *J. Min. Saf. Eng.* **2010**, *1*, 40–44.



© 2019 by the authors. Licensee MDPI, Basel, Switzerland. This article is an open access article distributed under the terms and conditions of the Creative Commons Attribution (CC BY) license (<http://creativecommons.org/licenses/by/4.0/>).